Supporting information for:

Long-Lived Triplet State in a Platinum(II) Perylene Monoimide Complex

James E. Yarnell[a], Arnab Chakraborty[a], Mykhaylo Myahkostupov[a], Katherine M. Wright[a], and Felix N. Castellano[a]*

[a] Department of Chemistry, North Carolina State University, Raleigh, North Carolina, 27695-8204, United States

CONTENTS:

1. Synthetic Procedures for Precursors

2. Additional Optical Spectra

3. Characterization Data for New Compounds

4. Additional DFT Results

1. Synthetic Procedures for Precursors

Synthesis of N-(2,5-di-tert-butylphenyl)-perylene-3,4-dicarboxylic imide (PMI). Perylene-3,4,9,10-tetracarboxylicanhydride (10.99 g, 0.028 mol), 2,5-di-*tert*-butyl-aniline (3.16 g, 0.015 mol), zinc acetate (1.32 g, 0.007 mol), imidazole (56.06 g, 0.823 mol), and water (24 g, 1.33 mol) were added to a pressure vessel and heated to 190 °C for 22 hours. After cooling to room temperature, the reaction mixture was filtered through a pad of celite and filter cake was washed with chloroform (3 x 300 mL). The combined filtrate was concentrated down washed with water (2 x 100 mL) and brine (50 mL). Organic layer was dried over sodium sulfate (anh.) and concentrated. The product was purified by silica gel chromatography using DCM as the eluent, followed by recrystallization via liquid diffusion using methanol/DCM to afford 2.3 g (16%) of PMI as dark red solid.

Synthesis of 9-bromo-N-(2,5-di-tert-butylphenyl)-perylene-3,4-dicarboxylic imide. *N*-bromosuccinimide (534 mg, 3.0 mmol) was added to a stirring solution of PMI (1.36 g, 2.67 mmol) in anhydrous DMF (90 mL) at room temperature under nitrogen. The reaction mixture was heated to 40 °C for 48 hours. After cooling to room temperature, the reaction mixture was poured into water (500 mL). The precipitated product was collected by filtration, washed with water (2 x 50 mL) and dried under vacuum to afford 1.04 g (66%) of PMI-Br as yellow solid.

Synthesis of 9-(trimethylsilylethynyl)-N-(2,5-di-tert-butylphenyl)-perylene-3,4-dicarboxylic imide (PMI-CCTMS). PMI-Br (420 mg, 0.714 mmol), Pd(PPh$_3$)$_4$ (120 mg, 0.104 mmol) and CuI (80 mg, 0.42 mmol) were added under nitrogen to a 1:1 mixture of anhydrous dichloromethane/diisopropylamine (60 mL) and purged with nitrogen for 15 minutes. Trimethylsilylacetylene (4.0 mL) was added, and the reaction mixture was heated to 60 °C for 36 hrs. After cooling to room temperature, volatiles were removed under vacuum, and the crude was purified by silica gel chromatography to afford PMI-CCTMS as orange solid in 90% yield (393 mg).

Synthesis of Dichlorobis(dimethyl-sulfoxide)platinum(II), Pt(DMSO)$_2$Cl$_2$. Potassium tetrachloroplatinate(II) (630 mg, 1.52 mmol) was dissolved in a mixture of DMSO (1.0 mL) and deionized water (10 mL), and the reaction mixture was stirred for 3 hours at room temperature. The precipitated product was collected by filtration, washed with deionized water (50 mL) and dried under vacuum tom afford an off-white solid in 80% yield (517 mg). The product was used in the next step without further purification.

Synthesis of chloro(4,4',4"-tri-tert-butyl-2,2':6',2"-terpyridine) platinum(II), [Pt(tbut$_3$-trpy)Cl](PF$_6$). Pt(DMSO)$_2$Cl$_2$ (250 mg, 0.59 mmol) was added to a solution of 4,4',4"-tri-*tert*-butyl-2,2':6',2"-terpyridine (262 mg, 0.65 mmol) in a mixture of dichloromethane/methanol (15 mL:30 mL), and the reaction mixture was refluxed for 24 hours (Scheme 2). The bright yellow solid was collected by filtration and dried under vacuum. The solid was then dissolved in methanol, followed by a dropwise addition of an aqueous solution of ammonium hexafluorophosphate (1.0 g in 10 mL) to precipitate the desired product. The solid was collected by filtration, washed with deionized water (100 mL) and dried under vacuum. The product was isolated with 93% yield (426 mg) and used without further purification. ^{1}H NMR (CD$_3$CN): 8.82 (d, 2H), 8.30 (s, 4H), 7.79 (d, 2H), 1.54 (s, 9H), 1.46 (s, 18H).
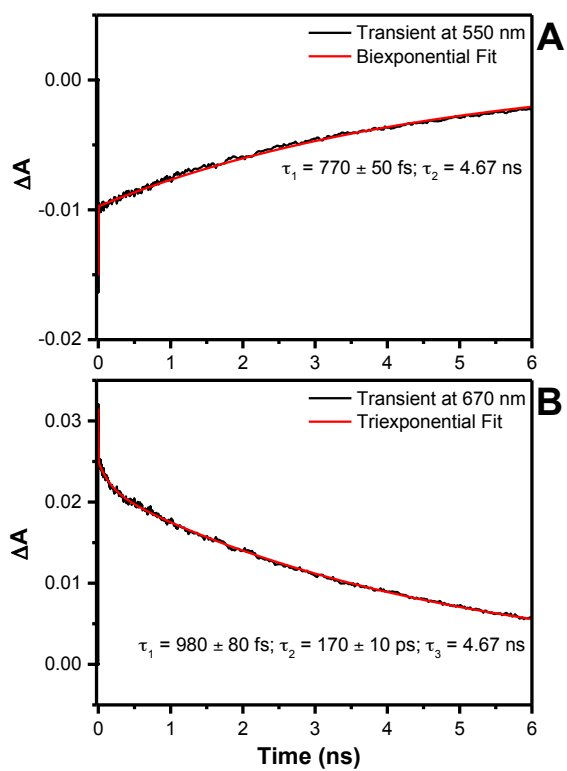
2. Additional Optical Spectra
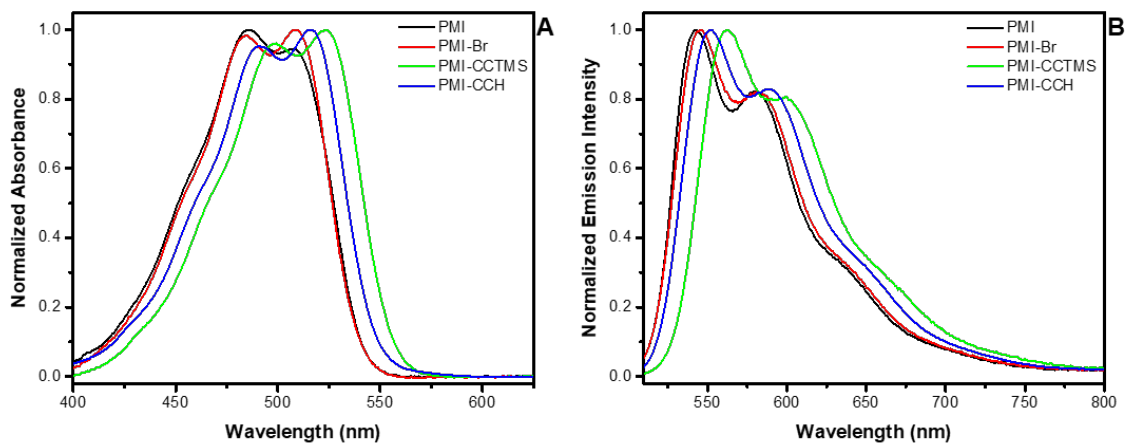
Figure S1. Normalized absorption (A) and photoluminescence (B) spectra of PMI, PMI-Br, PMI-CCTMS, and PMI-CCH in aerated dichloromethane.
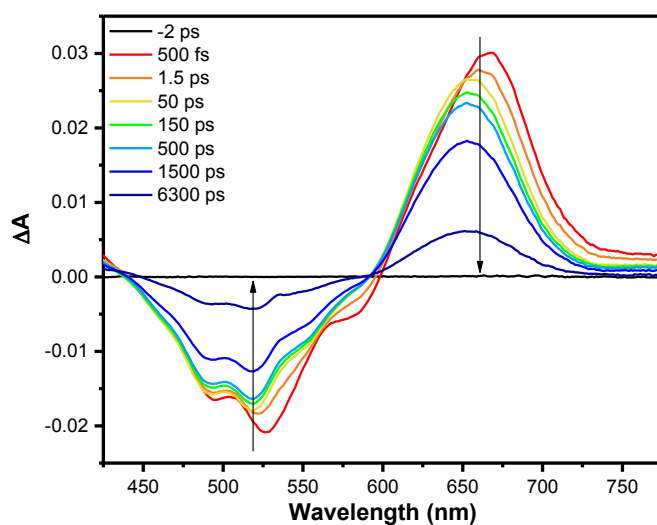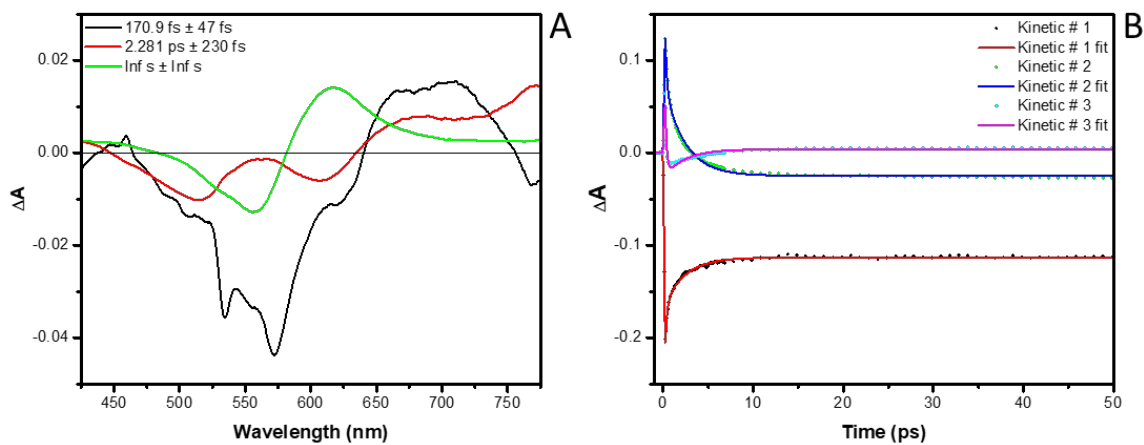

Figure S2. Excited-state absorption difference spectra of **1** in dichloromethane following 525 nm pulsed excitation (105 fs fwhm).
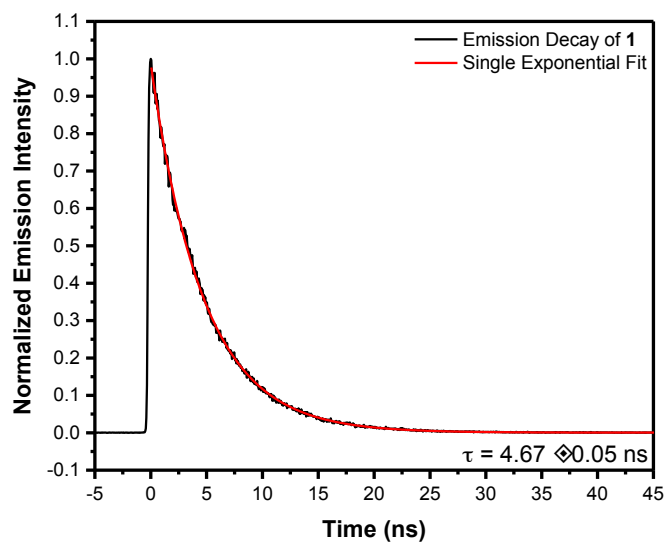
S3

Figure S3. Excited-state absorption single wavelength kinetic analysis at 550 nm (A) and single wavelength kinetic analysis at 670 nm (B) of **1** in dichloromethane following 525 nm pulsed excitation (105 fs fwhm).
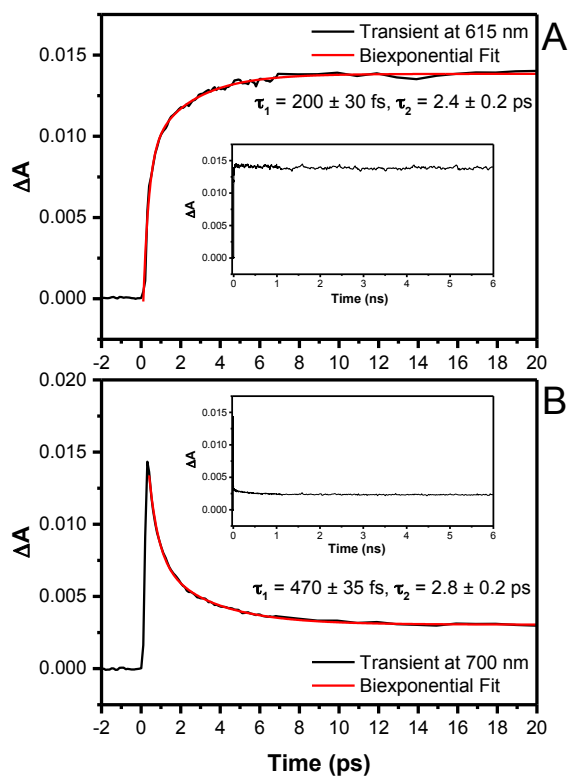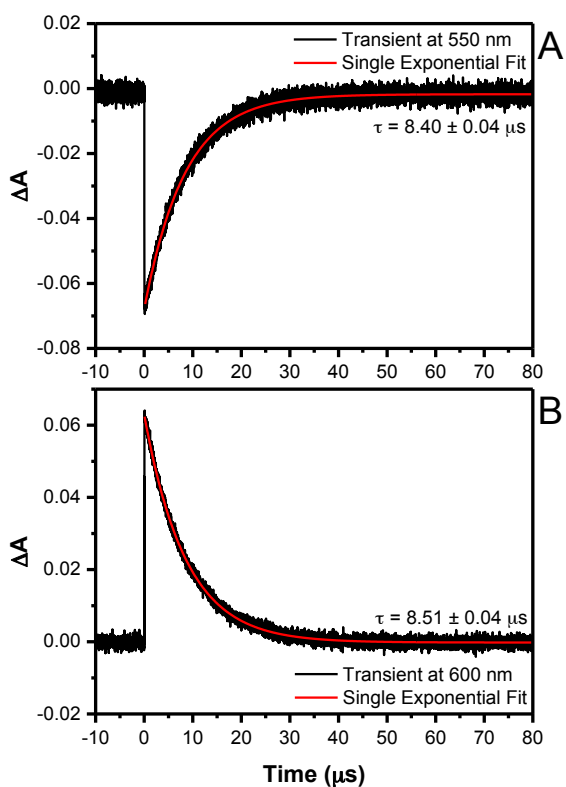
Figure S4. Excited-state absorption single wavelength kinetic analysis at 615 nm (A) and single wavelength kinetic analysis at 700 nm (B) of **2** in dichloromethane following 550 nm pulsed excitation (105 fs fwhm).


Figure S5. Ultrafast transient absorption kinetic data of **2** in dichloromethane following 550 nm pulsed excitation (105 fs fwhm). (A) Global fit spectral analysis of transient absorption data. (B) Global fit kinetic analysis of transient absorption data.

Figure S6. Time-resolved photoluminescence decay of **1** in dichloromethane following 525 nm pulsed excitation (7 ns fwhm).


Figure S7. Excited-state absorption single wavelength kinetic analysis at 550 nm (A) and single wavelength kinetic analysis at 600 nm (B) of **2** in dichloromethane following 530 nm pulsed excitation (7 ns fwhm).
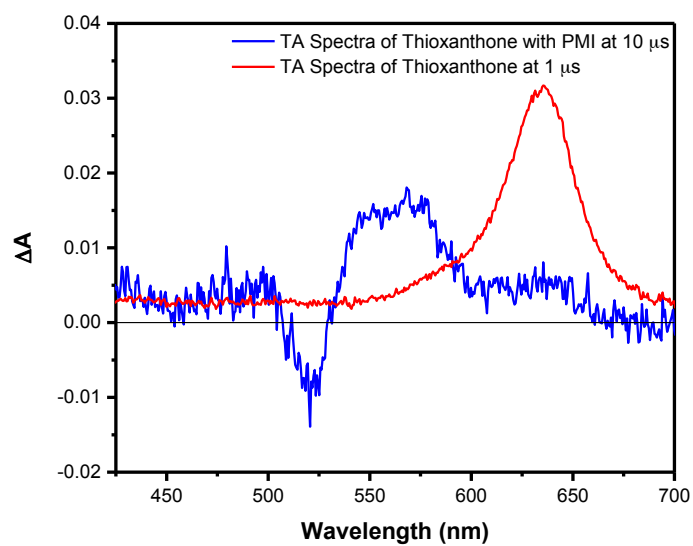
Figure S8. Excited-state absorption difference spectra of thioxanthone and thioxanthone with PMI (**1**) in dichloromethane following 380 nm pulsed excitation (7 ns fwhm). The PMI chromophore was sensitized by thioxanthone to observe the triplet spectra.
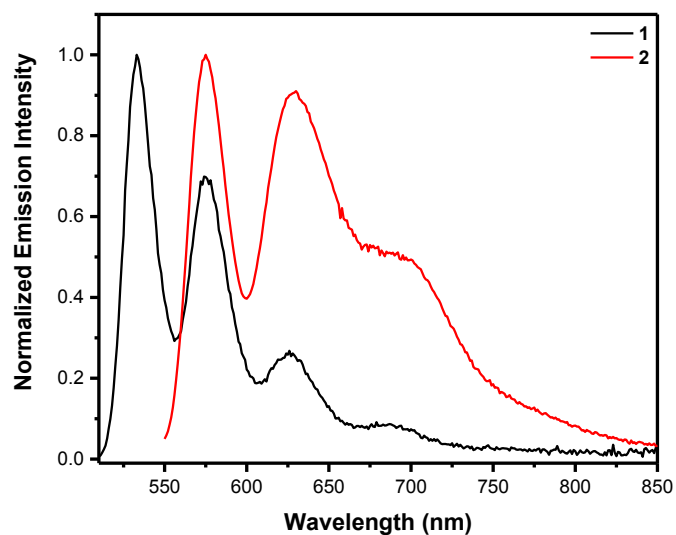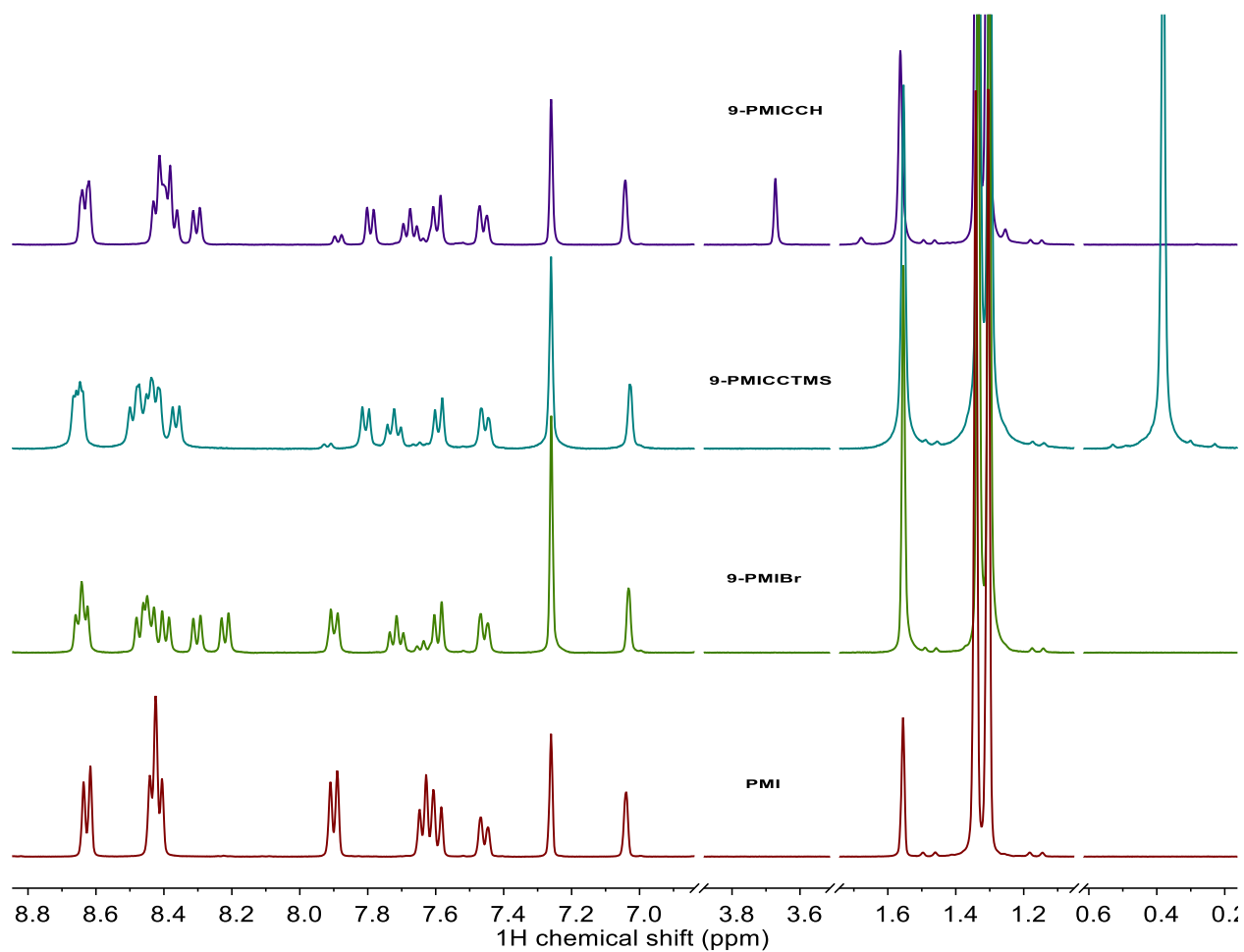

Figure S9. Photoluminescence spectra of **1** (black line) and **2** (red line) at 77 K in MTHF glasses (λ_{ex} = 500 nm).
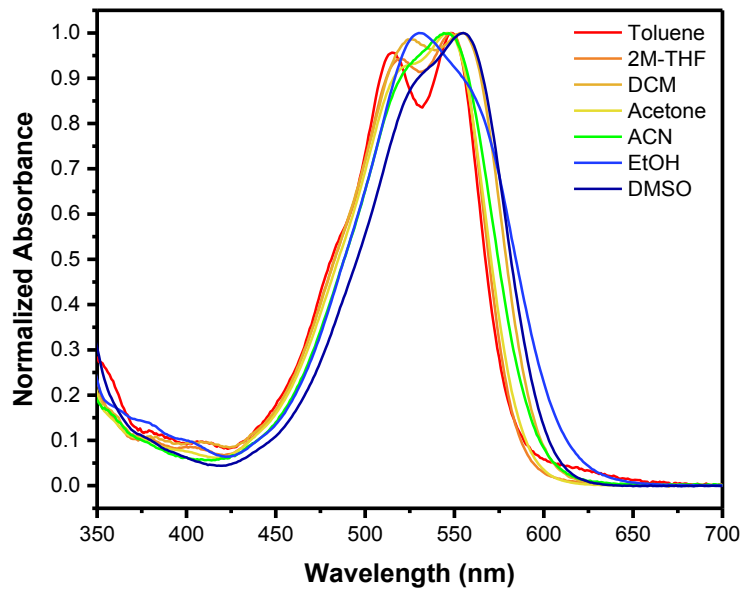
Figure S10. Normalized electronic spectra of **2** in various solvents.

3. Characterization Data for New Compounds

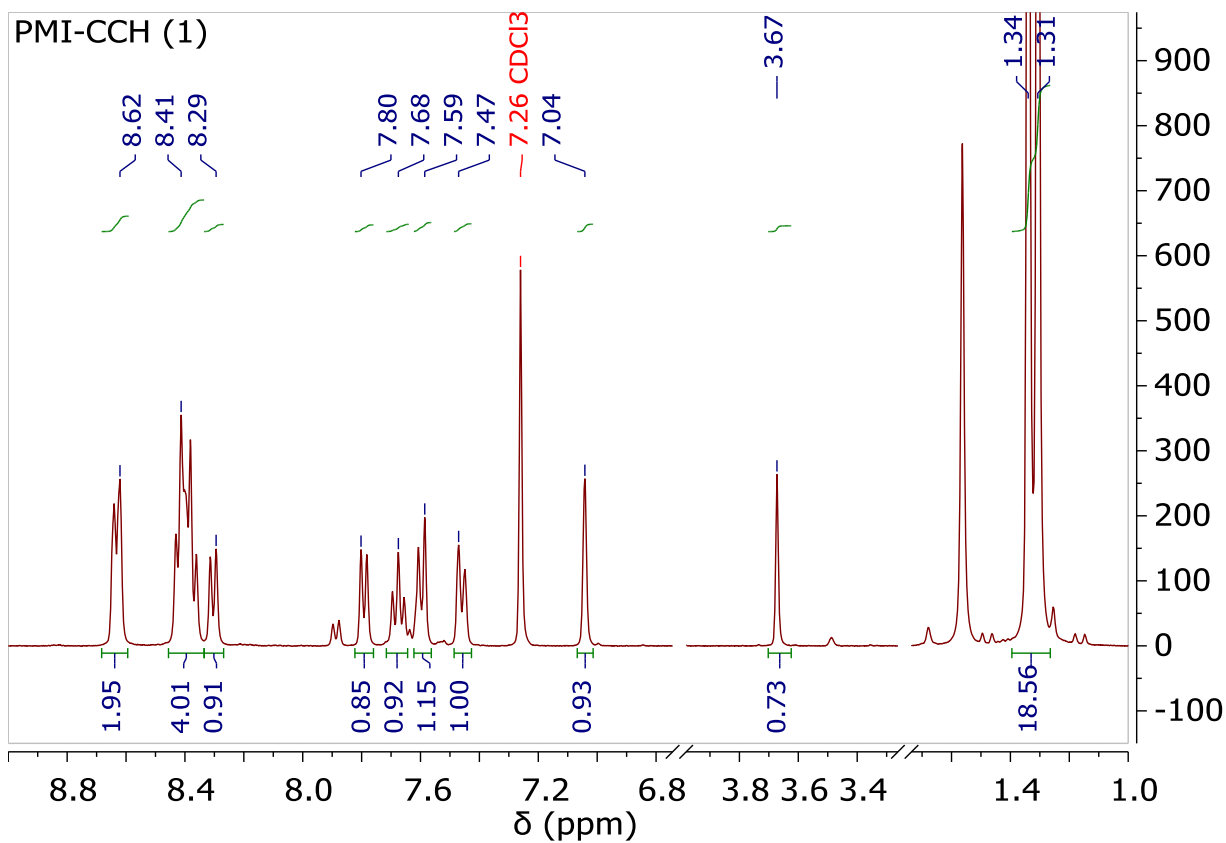**Figure S11**. ^{1}H NMR of PMI-CCH synthons in CDCl$_3$ (400 MHz).

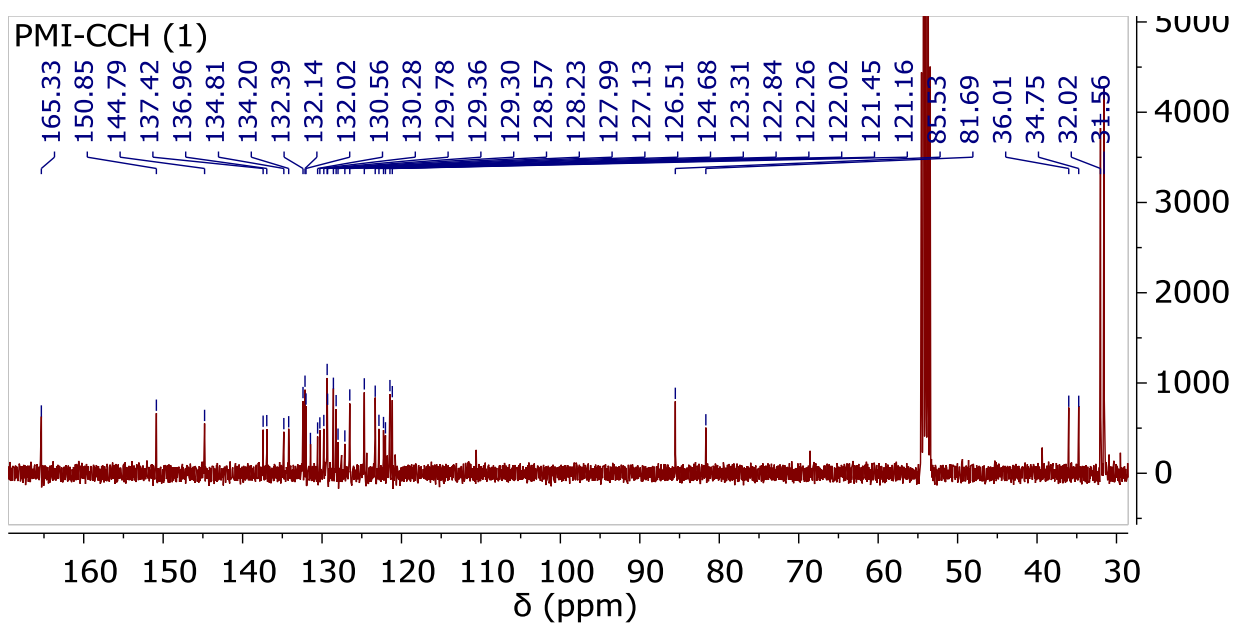**Figure S12**. ^{1}H NMR of PMI-CCH (**1**) in CDCl$_3$ (400 MHz).

Figure S13. ^{13}C NMR of PMI-CCH (**1**) in CD$_2$Cl$_2$ (100 MHz).
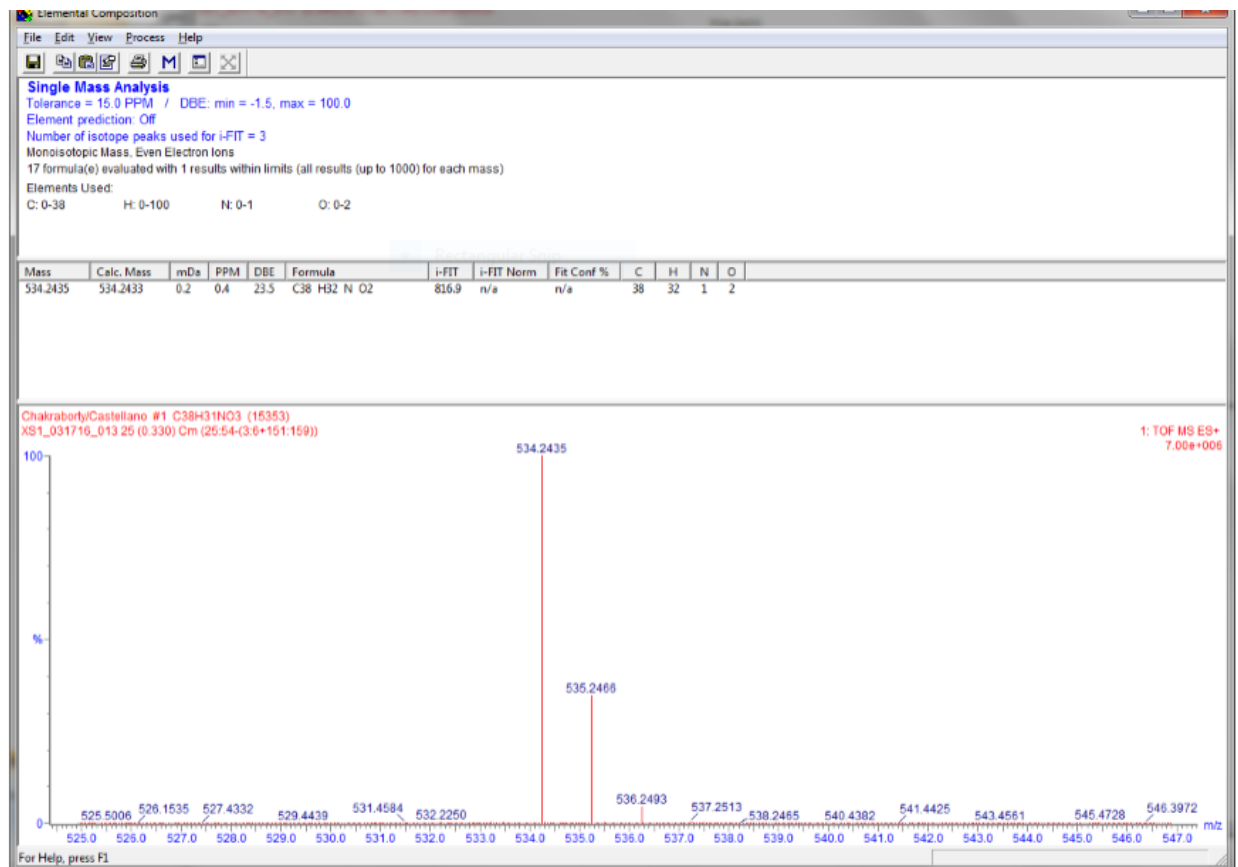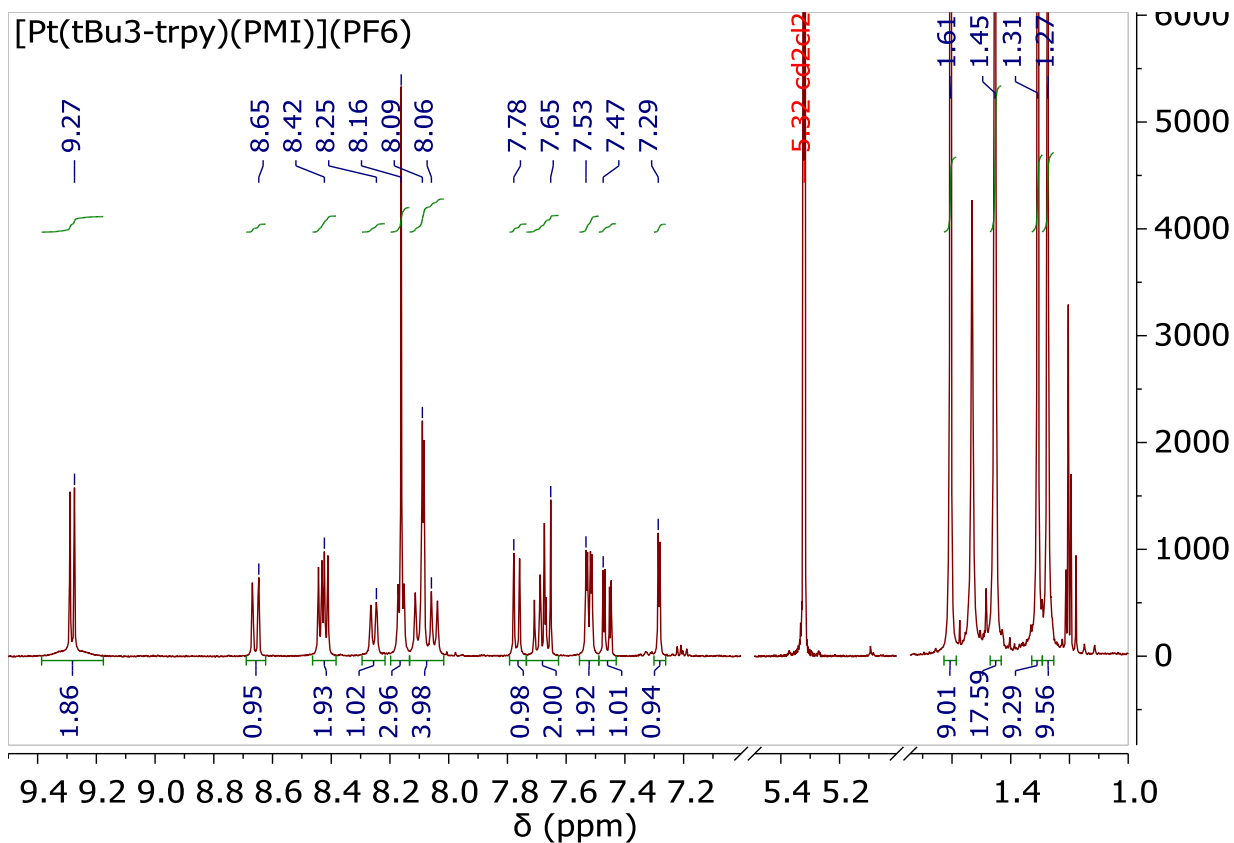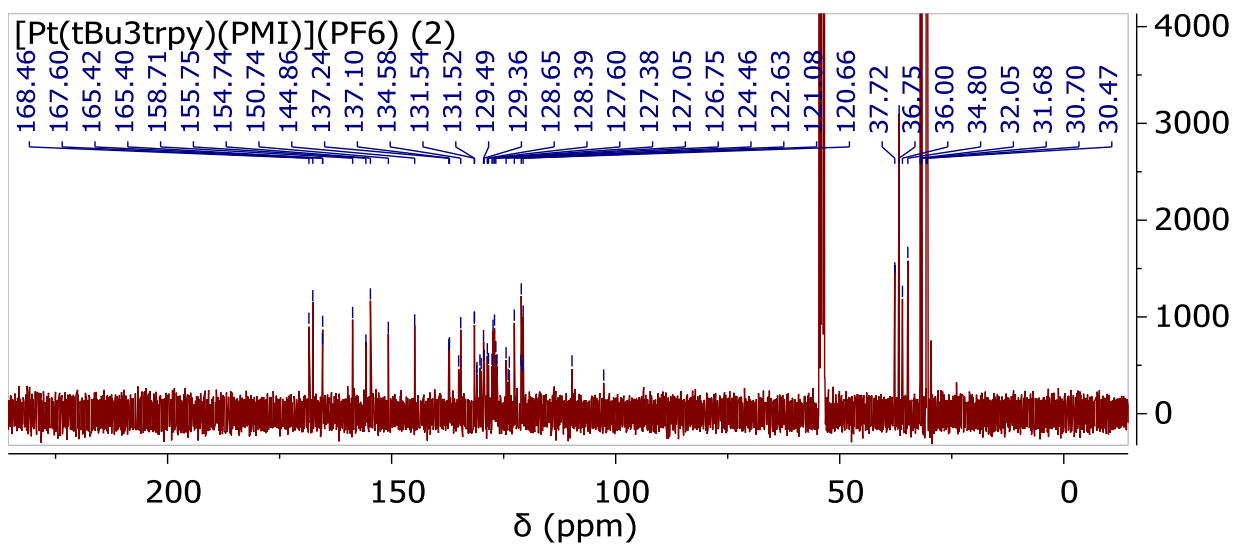

Figure S14. ESI-HRMS of PMI-CCH (**1**).

Figure S15. ^{1}H NMR of [Pt(tbut$_3$-trpy)PMI](PF$_6$) (**2**) in CD$_2$Cl$_2$ (400 MHz).

Figure S16. ^{13}C NMR of [Pt(tbut$_3$-trpy)PMI](PF$_6$) (**2**) in CD$_2$Cl$_2$ (100 MHz).
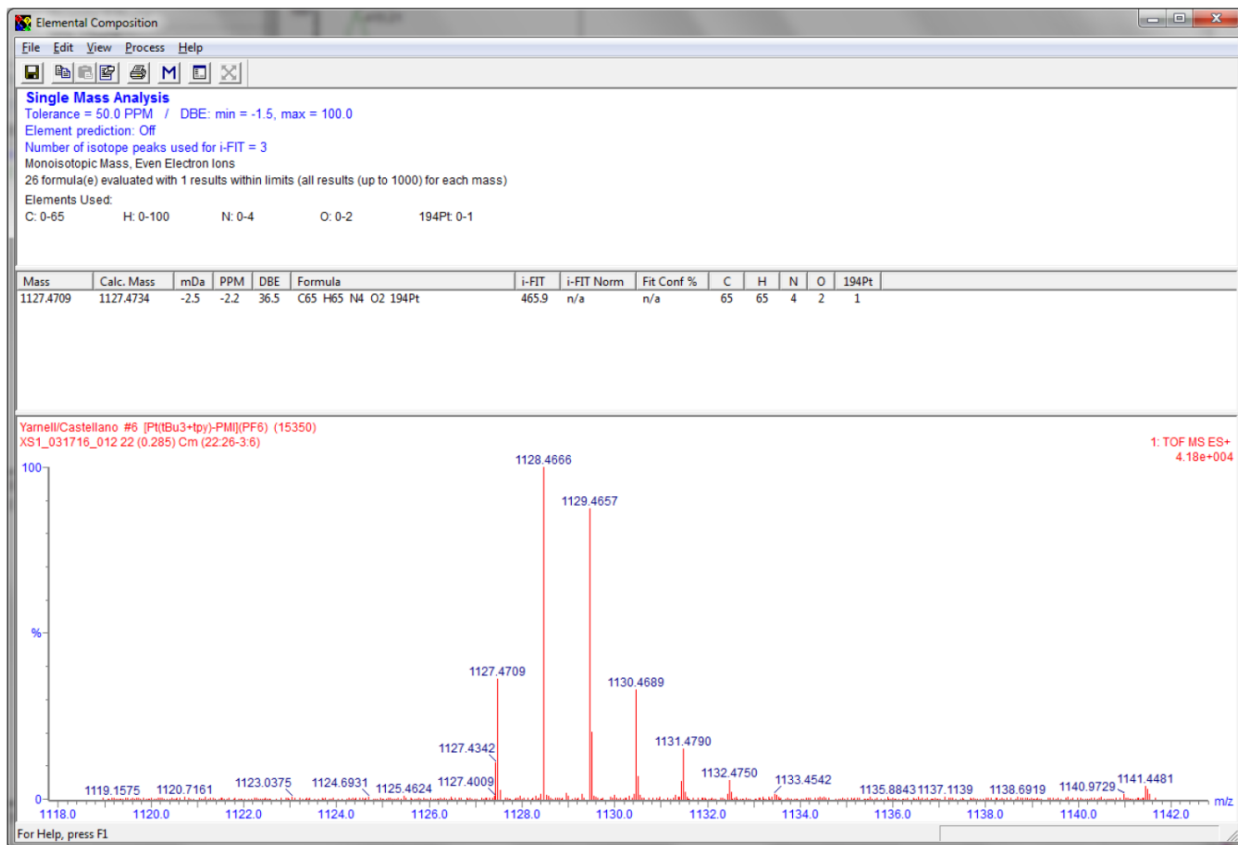
Figure S17. ESI-HRMS of [Pt(tbut$_3$-trpy)PMI](PF$_6$) (**2**).

Ground State

B3LYP-D3: -35.7°   CAM-B3LYP-D3: -38.8°

PBE0-D3: -38.5°   M06-D3: -40.8°
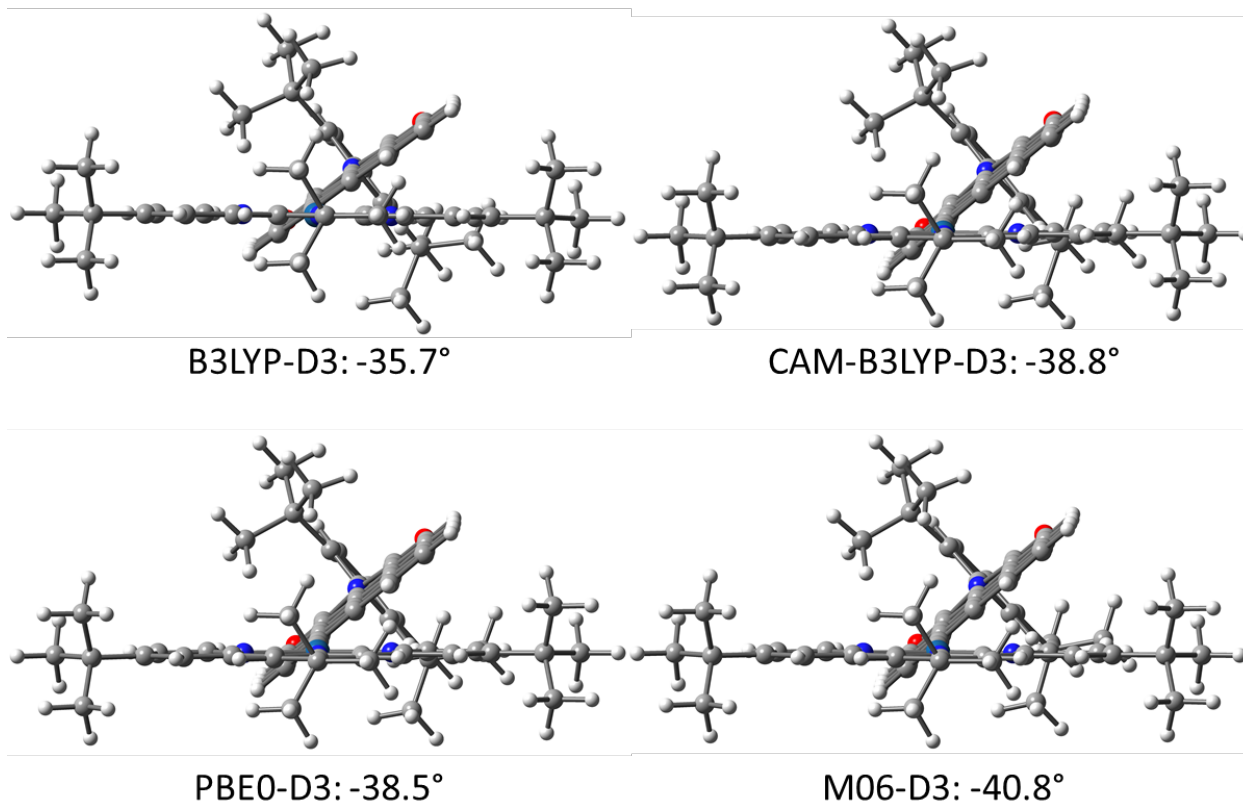
Figure S18. Optimized ground state geometries of [Pt(tbut$_3$-trpy)PMI](PF$_6$) (**2**) calculated using the functional specified with Def2-SVP basis set and SDD ECP. The geometries are aligned looking down the Pt(II) acetylide bond and the dihedral angle between the terpyridine and PMI aromatic systems are noted.

Triplet State

B3LYP-D3: -33.3°

CAM-B3LYP-D3: -36.0°

PBE0-D3: -35.0°

M06-D3: -39.9°
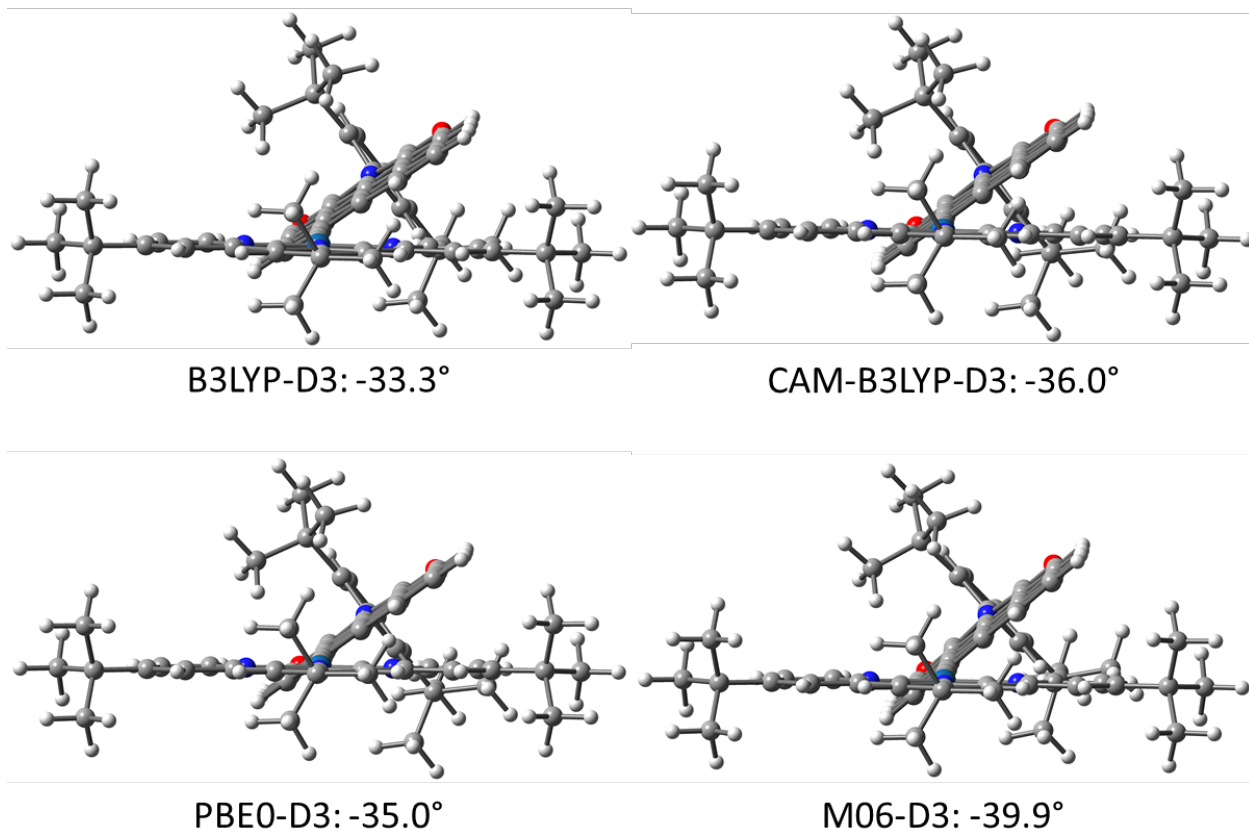
Figure S19. Optimized triplet state geometries of [Pt(tbut$_3$-trpy)PMI](PF$_6$) (**2**) calculated using the functional specified with Def2-SVP basis set and SDD ECP. The geometries are aligned looking down the Pt(II) acetylide bond and the dihedral angle between the terpyridine and PMI aromatic systems are noted.
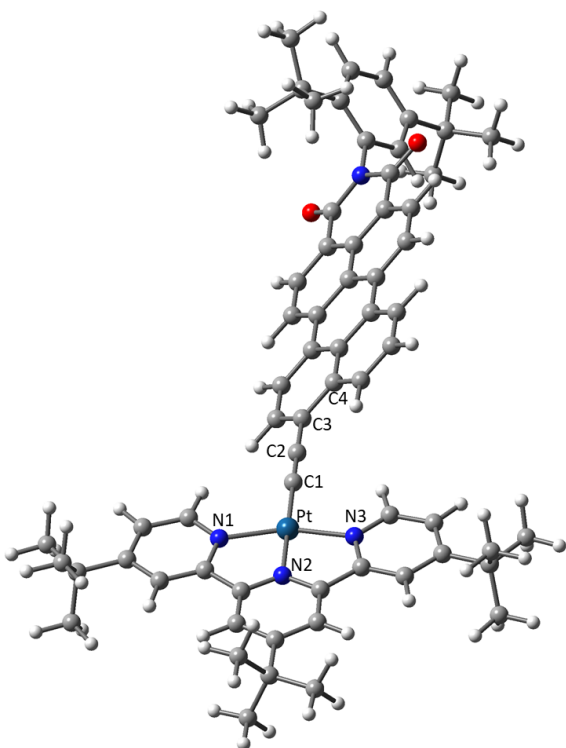
Ground State Geometry Around the Pt

	PBE0-D3	M06-D3	B3LYP-D3	CAM-B3LYP-D3
Pt-C1	1.963 Å	1.980 Å	1.978 Å	1.981 Å
Pt-N1	2.038 Å	2.063 Å	2.063 Å	2.053 Å
Pt-N2	1.983 Å	2.005 Å	2.004 Å	1.996 Å
Pt-N3	2.037 Å	2.063 Å	2.063 Å	2.052 Å
C1-C2	1.231 Å	1.231 Å	1.232 Å	1.223 Å
N1-Pt-N2	80.2°	79.7°	79.8°	80.0°
N1-Pt-N3	160.3°	159.3°	159.5°	159.8°
N3-Pt-C3-C4	-38.5°	-40.8°	-35.7°	-38.7°

Figure S20. The bond distances and angles around the Pt(II) using the optimized ground state geometry of [Pt(tbut$_3$-trpy)PMI](PF$_6$) (**2**) calculated using the functional specified with Def2-SVP basis set and SDD ECP.
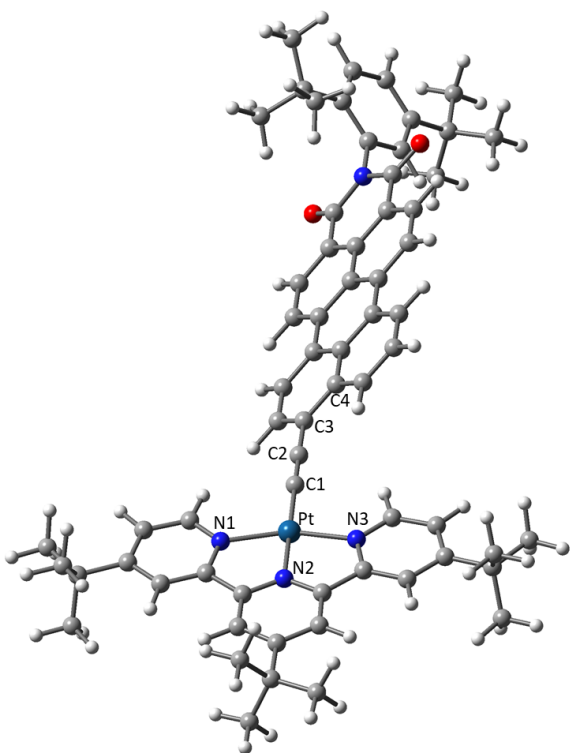
Triplet State Geometry Around the Pt

|	PBE0-D3	M06-D3	B3LYP-D3	CAM-B3LYP-D3
Pt-C1	1.959 Å	1.976 Å	1.973 Å	1.978
Pt-N1	2.038 Å	2.063 Å	2.063 Å	2.053
Pt-N2	1.982 Å	2.004 Å	2.003 Å	1.996
Pt-N3	2.037 Å	2.063 Å	2.063 Å	2.053
C1-C2	1.236 Å	1.236 Å	1.237 Å	1.228
N1-Pt-N2	80.2°	79.7°	79.8°	80.0
N1-Pt-N3	160.3°	159.3°	159.5°	159.8
N3-Pt-C3-C4	-35.0°	-39.9°	-33.3°	-36.0

Figure S21. The bond distances and angles around the Pt(II) using the optimized triplet state geometry of [Pt(tbut$_3$-trpy)PMI](PF$_6$) (**2**) calculated using the functional specified with Def2-SVP basis set and SDD ECP.

Table S1. Transition energies as determined via TDDFT using different functionals at the Def2-SVP/SDD level of theory.

Molecule	Functional	S$_0$ → S$_1$ (f)	S$_0$ → S$_2$ (f)
1	CAM-B3LYP	2.72 eV (1.0434)	3.92 eV (0.0031)
	M06	2.38 eV (0.9092)	3.26 eV (0.0000)
	PBE0	2.42 eV (0.9259)	3.21 eV (0.0000)
	B3LYP	2.24 eV (0.8915)	3.01 eV (0.0001)
2	CAM-B3LYP	2.60 eV (1.4664)	3.29 eV (0.0230)
	M06	2.16 eV (0.9540)	2.37 eV (0.3643)
	PBE0	2.14 eV (0.8690)	2.38 eV (0.4864)
	B3LYP	1.96 eV (0.5369)	2.25 eV (0.7763)

Table S2. T_1 energies as determined via TDDFT and ΔSCF at the M06-D3/Def2-SVP/SDD level of theory.

molecule	TDDFT (eV)	ΔSCF (eV)
1	1.26	1.28
2	1.23	1.26
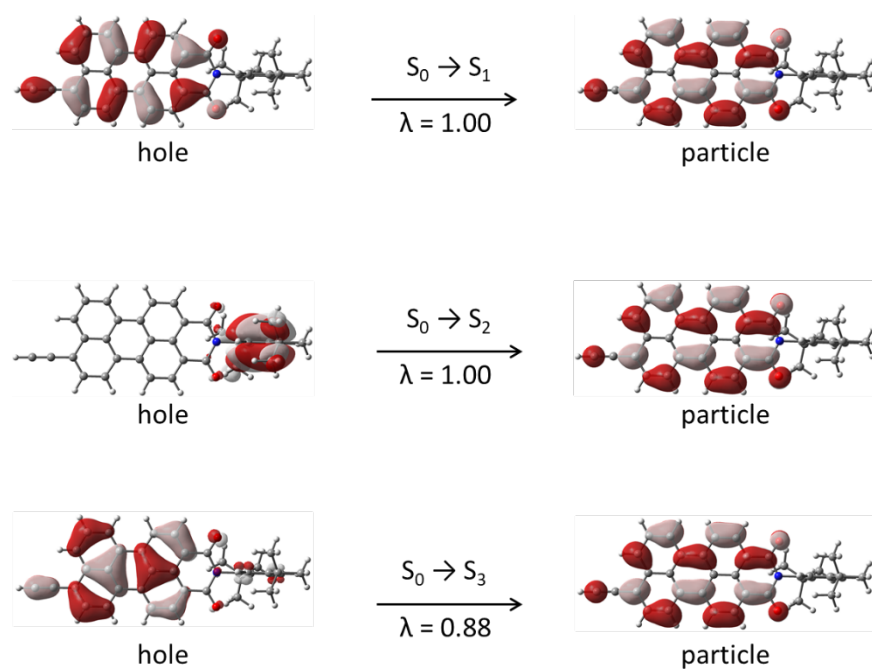
Figure S22. Natural transition orbitals (NTOs) for select $S_0 \rightarrow S_n$ excitations of **1** determined at the TD-DFT//M06-D3/Def2-SVP/SDD level of theory. λ is the fraction of the hole–particle contribution to the excitation.

Table S3. Calculated ground state and excited state (S_1) dipole moments as determined using different functionals at the Def2-SVP/SDD level of theory.

Molecule	Functional	S_0 Dipole (Debye)	S_1 Dipole (Debye)
1	CAM-B3LYP	6.387	9.609
	M06	7.216	9.636
	PBE0	6.966	9.718
	B3LYP	7.103	9.723
2	CAM-B3LYP	47.359	52.072
	M06	48.739	41.810
	PBE0	48.190	36.539
	B3LYP	48.497	24.711

Table S4. Calculated triplet state transition energies ($S_0 \rightarrow T_n$) as determined via

TD-DFT using different functionals at the Def2-SVP/SDD level of theory.

Molecule	Functional	$S_0 \rightarrow T_1$ (eV)	$S_0 \rightarrow T_2$ (eV)
1	CAM-B3LYP	1.190	2.660
	M06	1.257	2.603
	PBE0	1.185	2.577
	B3LYP	1.269	2.600
2	CAM-B3LYP	1.170	2.561
	M06	1.229	2.188
	PBE0	1.158	2.136
	B3LYP	1.229	1.945